JACS
JOURNAL OF THE AMERICAN CHEMICAL SOCIETY
Article
pubs.acs.org/JACS

Controlling the Size of Hot Injection Made Nanocrystals by Manipulating the Diffusion Coefficient of the Solute

Kim De Nolf,[†,‡,⊥] Richard K. Capek,*[,¶,⊥] Sofie Abe,[†,‡] Michael Sluydts,[§] Youngjin Jang,[¶] José C. Martins,[∥] Stefaan Cottenier,[§] Efrat Lifshitz,[¶] and Zeger Hens*[,†,‡]

[†]Physics and Chemistry of Nanostructures, [‡]Center for Nano and Biophotonics, [§]Center for Molecular Modeling, and [∥]NMR and Structural Analysis Unit, Ghent University, 9000 Gent, Belgium

[¶]Technion - Israel Institute of Technology, Haifa 3200003, Israel

Supporting Information

ABSTRACT: We investigate the relation between the chain length of ligands used and the size of the nanocrystals formed in the hot injection synthesis. With two different CdSe nanocrystal syntheses, we consistently find that longer chain carboxylic acids result in smaller nanocrystals with improved size dispersions. By combining a more in-depth experimental investigation with kinetic reaction simulations, we come to the conclusion that this size tuning is due to a change in the diffusion coefficient and the solubility of the solute. The relation between size tuning by the ligand chain length and the coordination of the solute by the ligands is further explored by expanding the study to amines and phosphine oxides. In line with the weak coordination of CdSe nanocrystals by amines, no influence of the chain length on the nanocrystals is found, whereas the size tuning brought about by phosphine oxides can be attributed to a solubility change. We conclude that the ligand chain length provides a practical handle to optimize the outcome of a hot injection synthesis in terms of size and size dispersion and can be used to probe the interaction between ligands and the actual solute.

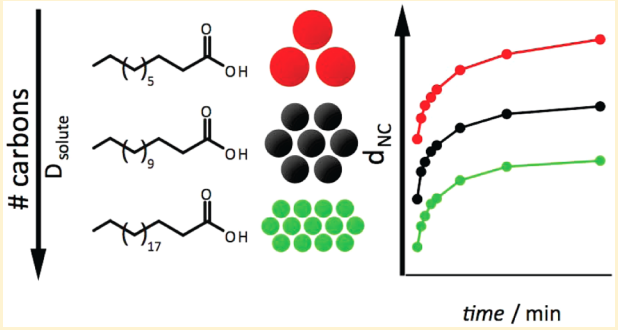

INTRODUCTION

Over the last 20 years, the hot injection synthesis has become a well-established method for the formation of monodisperse, sterically stabilized colloidal nanocrystals.[1] In general, the method is based on the initiation of a homogeneous nucleation and growth process by the rapid injection of one or more precursors into an apolar reaction mixture at elevated temperature.[2] Complexing agents or ligands are added, which help dissolve the precursors and stabilize the resulting colloid by steric hindrance. Initially developed for making cadmium chalcogenide nanocrystals,[3,4] it has been extended to the formation of a wide range of semiconductor, metal, and metal oxide nanocrystals. Key assets of the method are the excellent control over nanocrystal size, the narrow size dispersion of the colloids made, and the possibility—at least in some cases—to tune the shape.[5,6] In addition, an extremely versatile postprocessing methodology has been established, involving the further chemical modification to form heteronanostructures[7] or adjust the surface chemistry and the formation of monolayers, thin films, or superlattices by wet deposition techniques.[1]

Following the widespread use of colloidal nanocrystals as a model system to explore and understand the properties of nanoscale materials and their implementation as active material in various applications, the reaction mechanism of hot injection syntheses has become an active field of study. This involves both the question as to how precursors convert into a precipitant or solute (also called the growth species or monomer) and how the reaction chemistry is related to the development of the size and size dispersion of the nanocrystals throughout the reaction.[8−10] Importantly, such studies can provide a framework for rationalizing the reaction conditions, such as the choice and the concentration of the precursors and the functional headgroup, chain length, and concentration of the ligands. In some specific cases, including syntheses for PbSe, CdSe, and InP nanocrystals,[11−13] detailed chemical analysis has given insight in the precursor conversion chemistry. On the other hand, kinetic reaction simulations and extensive experimental studies on CdSe and CdS nanocrystal formation showed how the rate of precursor conversion is related to the size the nanocrystals attain at the end of the reaction.[14,15] Using the same combination of reaction simulations and an experimental study, it was demonstrated that the often reported increase of the nanocrystal diameter with increasing carboxylic acid concentration—an often used complexing agent—is due to an enhancement of the solute solubility.[16] Importantly, this implies that adjusting the carboxylic acid concentration, opposite from the precursor conversion rate, allows for size tuning at constant reaction rate.

Received: September 26, 2014
Published: January 28, 2015

DOI: 10.1021/ja509941g
J. Am. Chem. Soc. 2015, 137, 2495−2505

Considering that the solubility of saturated carboxylic acids in apolar solvents decreases with increasing chain length,[17] one could expect a comparable dependence of the nanocrystal diameter on the ligand chain length. In fact, a number of studies indicate that changing the chain length of the complexing agents, such as carboxylic acids, amines, phosphines, or phosphine oxides, provides indeed a versatile and straightforward method to change nanocrystal sizes. In the case of semiconductor nanocrystals, it has been demonstrated that for InP nanocrystals synthesized in the presence of a carboxylic acid, longer chain ligands yield smaller nanocrystals,[18,19] while similar observations have been made for other nanocrystal/ligand combinations such as PbSe,[20] CdS,[21] CdSe/carboxylic acid,[22] and CdSe/amine.[23] Moreover, the same principle has been applied for size tuning in the synthesis of metal and metal oxide nanocrystals, including Co/phosphine,[24] Ag/phosphine oxide,[25] and SnO_2/amine.[26] Although the observation that longer chained ligands yield smaller nanocrystals seems quite general, no satisfactory interpretation exists. Most often, it is assumed that this effect reflects a slowing down of the nanocrystal growth rate with increasing chain length due to steric hindrance within the ligand shell.[18,21,26] However, since the growth rate, i.e., the amount of material formed per unit of time, is eventually determined by the rate of solute formation, this interpretation seems flawed, and a more in-depth analysis is needed to understand the link between the ligand chain length and the diameter attained by the nanocrystals at the end of the reaction.

In this work, we use the quantitative analysis of two different syntheses of CdSe nanocrystals to address the influence of the ligand chain length on the nanocrystal diameter at the end of the reaction. The first is based on the hot injection of trioctylphosphine selenide in a mixture composed of a cadmium carboxylate, excess carboxylic acid and primary amines,[27,28] and the second involves the injection of selenium powder in a reaction mixture only composed of a cadmium carboxylate and excess carboxylic acid, all dissolved in octadecene.[22] In line with literature, we find that longer carboxylic acids lead to smaller nanocrystals with a better size dispersion. However, opposite from the idea that this results from a reduction of the reaction rate, we show that varying the carboxylic acid chain length leaves the reaction rate unchanged. By combining an experimental study involving carboxylic acid mixtures and previously developed kinetic reaction simulations,[15,16] we show that this size tuning at constant reaction rate is due to a change in solubility and diffusion coefficient of the growth species. The idea that the influence of the ligand chain length on the nanocrystal diameter is due to interaction between the ligand and the growth species is elaborated further by addressing the influence of the chain length of primary amines and phosphine oxides when added to the synthesis. Also in this case, we find that the reaction rate is unchanged when the chain length of any of the additives is varied. However, whereas increasing the chain length of the carboxylic acids or phosphine oxides again reduces the nanocrystal diameter, it follows that amines have little effect, if any, on the nanocrystal diameter. In particular the difference between carboxylic acids and amines is in line with the different complexation of CdSe nanocrystals by carboxylates (tightly bound) compared with amines (loosely bound, dynamic). We thus conclude that varying the ligand chain length in the hot injection synthesis is not only a straightforward method to tune the nanocrystal diameter and optimize size dispersions but also a sensitive probe to monitor the interaction between the ligand and the actual solute.

RESULTS AND DISCUSSION

Carboxylic Acids with Longer Hydrocarbon Chains Lead to Smaller Nanocrystals with Sharper Size Distributions. To investigate the effect of the ligand chain length in the hot injection synthesis, we used two different syntheses for CdSe nanocrystals. Both make use of a cadmium carboxylate as the Cd precursor, whereas the Se precursor is either trioctylphosphine selenide (TOPSe)[15,27,28] or a suspension of black selenium powder in octadecene (ODE).[22] Here, we run both syntheses using saturated carboxylic acids with different chain lengths to analyze the reaction rate and the nanocrystal diameter reached at the end of the reaction, where both syntheses are denoted as CdSe/TOPSe and CdSe/black Se, respectively.

Figure 1 summarizes the key properties of the CdSe/TOPSe synthesis. In practice, it involves the injection of TOPSe in a mixture of a cadmium carboxylate ($Cd(CA)_2$), excess carboxylic acid (CA), and hexadecylamine (HDA) in octadecene (ODE) in a 10:1:4:8 ratio of TOPSe:$Cd(CA)_2$:total CA:HDA, where we use either behenic (BAc, C22), myristic (MAc, C14) or decanoic acid (DAc, C10) as the carboxylic acid. As shown in

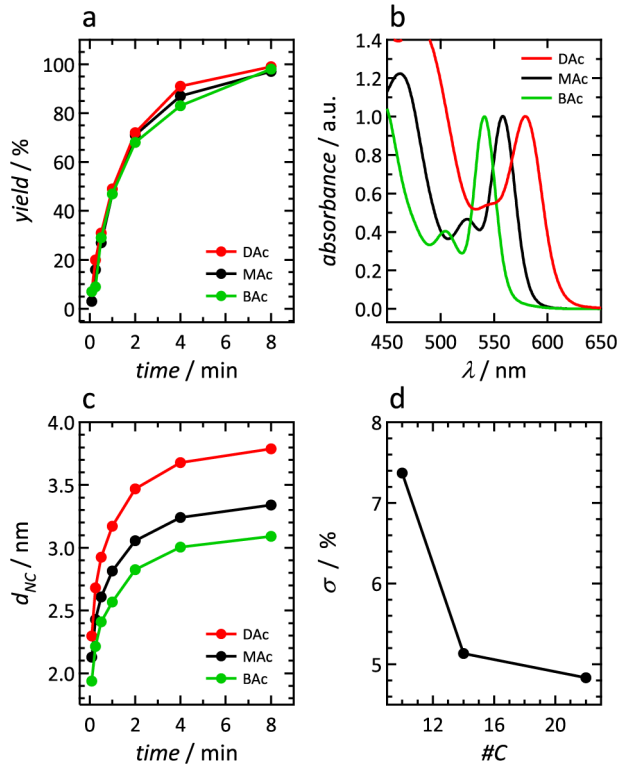

Figure 1. (a) Yield development of the CdSe/TOPSe synthesis using (green) behenic, (black) myristic and (red) decanoic acid as the carboxylic acid. (b) Absorption spectra recorded on aliquots taken 8 min after injection for the three different acids used (same color coding is in (a)). (c) Development of the diameter of CdSe nanocrystals during the same syntheses as shown in (a). (d) Size dispersion of the CdSe nanocrystals obtained 8 min after injection, plotted as a function of the amount of carbon atoms in the carboxylic acid chain. See Methods Section for synthesis details and the determination of the reaction yield and the nanocrystal diameter and size dispersion.

DOI: 10.1021/ja509941g
J. Am. Chem. Soc. 2015, 137, 2495−2505

the Supporting Information (Section S1), we analyze these reactions by means of the absorption spectra of aliquots taken at different times after the injection. Using the absorbance at short wavelength and the position λ_{1s-1s} of the first exciton peak, this provides us with the reaction yield and the mean nanocrystal diameter d_{NC}.[29] Figure 1a shows that irrespective of the acid chain length, the reaction yield reaches 90−100% after 8 min of reaction time, where also the overall time development appears chain-length independent. Clearly, this indicates that a change of the acid chain length does not slow down nor accelerate the reaction. On the other hand, the absorption spectra recorded on aliquots taken at 8 min after the injection show that shortening the carboxylic acid chain-length results in a progressive increase of λ_{1s-1s} (Figure 1b). This corresponds to larger nanocrystals for shorter chain lengths, a trend that holds in fact for all reaction times (Figure 1c). In addition, as shown in Figure 1d, also the size dispersion, which we estimate from the width of the first exciton transition, tends to increase when the acid chain length is reduced, especially for the shortest chain length used.

As shown in Figure 2, similar results are obtained with the CdSe/black Se synthesis, where black selenium powder is injected in a hot mixture of ODE, a cadmium carboxylate and excess carboxylic acid (see Supporting Information, Section S1, for the corresponding absorption spectra). Once more, syntheses using BAc, MAc, and DAc are compared. Figure 2a confirms that the reaction yield, reaching a final value of ≈45−50% within 4−8 min for these reactions carried out at respective injection/growth temperatures of 250/240 °C, is independent of the carboxylic acid used in this case as well. In addition, shorter chain lengths lead again to larger nanocrystals (see Figure 2b,c), whereas especially in the case of DAc, a considerable deterioration of the width of the first exciton transition is observed (see Figure 2d). At more elevated injection/growth temperatures of 270/260 °C, a similar behavior is observed, where the size dispersion for the shortest ligand used (DAc) deteriorates even further due to nanocrystal fusion in the final stage of the reaction (see Supporting Information, Section S2). We thus conclude that longer-chained carboxylic acid ligands in colloidal hot injection synthesis lead to ensembles of smaller particles with sharper size distributions.

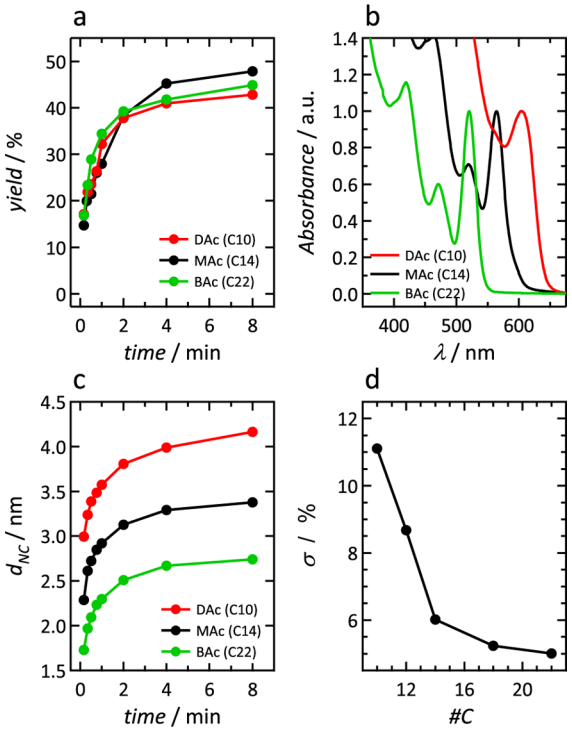

Figure 2. (a) Yield development of the CdSe/black Se synthesis using (green) behenic, (black) myristic, and (red) decanoic acid as the carboxylic acid using injection/growth temperatures of 250/240 °C, respectively. (b) Absorption spectra recorded on aliquots taken 8 min after injection for the three different acids used (same color coding as in (a)). (c) Development of the diameter of CdSe nanocrystals during the same syntheses as shown in (a). (d) Size dispersion of the CdSe nanocrystals obtained 8 min after injection, plotted as a function of the amount of carbon atoms in the carboxylic acid chain. See Methods Section for synthesis details and the determination of nanocrystal diameter.

Final Nanocrystal Diameter Follows the Average Numbers of Carbon Atoms in a Carboxylic Acid Mixture. To further investigate the dependence of the nanocrystal diameter and size dispersion on the acid chain length, we performed the CdSe/black Se synthesis using mixtures of carboxylic acids. This involved the combination of saturated carboxylic acids with oleic acid (OAc) while keeping the overall acid concentration constant. Figure 3a indicates that these reactions feature the same yield development, reaching a constant yield of ≈70% within 2−4 min. The respective absorption spectra of aliquots taken after a reaction time of 8 min for syntheses performed using mixtures of DAc, MAc, and BAc with OAc in a 1:1 ratio are shown in Figure 3b. Again, we find that replacing BAc by MAc and DAc in the mixture leads to a reduction of λ_{1s-1s} (and thus d_{NC}). Moreover, λ_{1s-1s} obtained for a carboxylic acid mixture of DAc (C10) and OAc (C18, unsaturated) nearly coincides with λ_{1s-1s} obtained using only MAc (C14), whose number of carbon atoms is the average of that of DAc and OAc (see Figure 3c). The same conclusion holds for λ_{1s-1s} attained with the other acid mixtures, which almost perfectly fit the trend line obtained by syntheses with a single, saturated carboxylic acid only. Finally, also in terms of size dispersion, the outcome of reactions using carboxylic acid mixtures strongly resembles the results obtained using a single saturated acid with an equivalent number of carbon atoms (see Figure 3d). Hence, we conclude that the final diameter of the NCs mainly depends on the average chain length of the carboxylic acid mixture used.

Size Tuning by Varying the Carboxylic Acids Chain Length Is Governed by the Takeover of Nucleation by Growth. In the mechanistic picture put forward for nanocrystal syntheses such as the CdSe/TOPSe reaction, the precursors first react to form the solute or monomer species that is then used to nucleate and grow CdSe nanocrystals. Next to detailed molecular studies that have appeared in the literature,[11−13] a strong argument supporting this view is the finding that the same yield development is obtained under reaction conditions where the concentration and the size of the nanocrystals is different.[15] This behavior is confirmed in this study for both the CdSe/TOPSe and CdSe/black Se synthesis, which brings us to the conclusion that in both cases, the rate of nucleation and growth of nanocrystals is set by the rate of solute formation. Under these conditions, nanocrystals with different sizes can be obtained by shifting the point where the solute consumption by nanocrystal growth overtakes the solute consumption by

DOI: 10.1021/ja509941g
J. Am. Chem. Soc. 2015, 137, 2495−2505

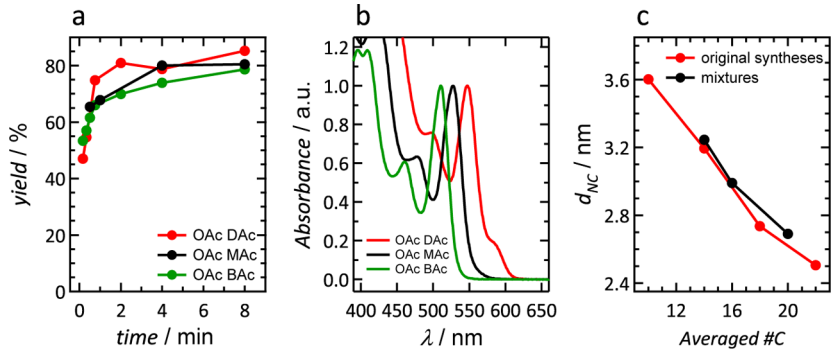

Figure 3. (a) Yield development of the CdSe/black Se synthesis using 1:1 mixtures of (green) behenic, (black) myristic, and (red) decanoic acid with OAc using injection/growth temperatures of 270/260 °C, respectively. (b) Absorption spectra recorded on aliquots taken 8 min after injection for the three different acid mixtures used (same color coding as in (a)). The long wavelength shoulder in the OAc-DAc spectra is due to nanocrystal fusion (see Supporting Information, Section S2) (c) Diameter attained after 8 min of reaction time for (black markers) CdSe/black Se syntheses using a single saturated carboxylic acid and (red markers) 1:1 mixtures of a saturated carboxylic acid and OAc as a function of the average number of carbon atoms of the carboxylic acids. See Methods Section for synthesis details and the determination of nanocrystal diameter.

nucleation.[16] Hence the question as to how the ligand chain length affects this takeover.

To analyze this question, we start from established expressions for the rate of nanocrystal nucleation J_N (i.e., the number of nuclei formed per second) and nanocrystal growth j_G (i.e., the change of the NC radius per second). Both depend on parameters such as the diffusion coefficient D of the solute, the volume of a solute molecule v_0, the surface tension γ, the molar volume V_m of the material formed, the nanocrystal radius r, the rate constants k_g^∞ and k_d^∞ for solute adsorption and desorption, the transfer coefficient α for solute adsorption and the supersaturation S, which is defined as the ratio between the actual concentration and the solubility $[M]_0$ of the solute:[30]

$$J_N = \frac{2D}{v_0^{5/3}} \exp\left(-\frac{16\pi\gamma^3 V_m^2 N_A}{3(RT)^3(\ln S)^2}\right) \quad (1)$$

$$j_G = DV_m[M]_0\left[\frac{S - \exp\left(-\frac{2\gamma V_m}{rRT}\right)}{r + \frac{D}{k_g^\infty}\exp\left(\alpha\frac{2\gamma V_m}{rRT}\right)}\right] \quad (2)$$

To understand how the different variables in these expressions influence d_{NC} at constant reaction rate, we consider a point in time right after the start of the reaction, where little or no nanocrystals have been formed. Under these conditions, all solute species generated are to be consumed by nucleation. Writing the initial rate of solute formation as $G_{M,0}$, one can thus write:

$$G_{M,0} = \frac{4\pi r_c^3}{3}\frac{N_A}{V_m}J_N \quad (3)$$

Here, r_c is the critical radius, i.e., the radius at which nuclei are stable for the prevailing supersaturation:

$$r_c = \frac{2\gamma V_m}{RT\ln S} \quad (4)$$

When the reaction rate is constant, $G_{M,0}$ will be constant as well and thus also the product of J_N and the volume of the critical nuclei. Given the relation between r_c and S, this means that the initial supersaturation will depend on both D, i.e., more in general, the nucleation rate prefactor, and γ. According to eq 1, increasing the prefactor will raise the nucleation rate while increasing γ will lower it. Since $G_{M,0}$ must remain fixed, these changes of parameters must be offset by a change of the supersaturation. In this respect, a variation of S has a much stronger influence on J_N , where S affects the exponent, than on r_c. As a result, an increase of the nucleation rate prefactor will lower S while increasing the surface tension will increase S. Using eq 2, one sees that an increase of the supersaturation leads to a faster nanocrystal growth and thus a faster takeover of nucleation by growth. As summarized in Table 1, this makes that an increase of the nucleation prefactor results in smaller nanocrystals, while a larger surface tension will increase d_{NC}. Alternatively, parameters like D, $[M]_0$, or k_g^∞ can directly influence the growth rate. Again, an increase of the growth rate will expedite the takeover of nucleation by growth. As summarized in Table 1, this implies that an increase of D, $[M]_0$, or k_g^∞ will lead to larger nanocrystals at the end of the reaction.

Table 1. Overview of the Different Adjustable Parameters in the Expression for the Nucleation Rate J_N (eq 1) and the Growth Rate j_G (eq 2)[a]

variable	change analyzed	effect on J_N	effect on j_G	effect on d_{NC}	effect on σ_d
D - prefactor	↑	↑	–	↓	–
γ	↑	↓	–	↑	↓
k_g^∞	↑	–	↑	↑	↓
D - growth rate	↑	–	↑	↑	↑
$[M]_0$	↑	–	↑	↑	↑

[a]When increasing these parameters, arrows up or down indicate an ensuing increase or decrease of J_N, j_G, the nanocrystal diameter d_{NC}, and the size dispersion σ_d. These qualitative statements are corroborated by reaction simulations summarized in the Supporting Information (Section S3).

Importantly, the qualitative statements made in Table 1 can be confirmed by using eqs 1 and 2 to simulate the whole reaction development (see Supporting Information, Section S2). For all the parameters included in Table 1, the examples of these simulations are shown in the Supporting Information (Section S3). Moreover, considering the different parameters introduced, one can expect γ, k_d^∞ and k_g^∞ to be directly influenced by the composition and the dynamical properties of the nanocrystal ligand, whereas $[M]_0$ and D will be properties of the solute. This makes it possible to link the experimentally

DOI: 10.1021/ja509941g
J. Am. Chem. Soc. 2015, 137, 2495−2505

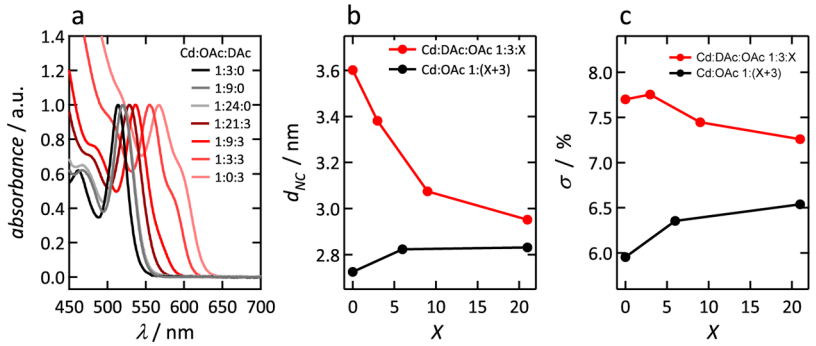

Figure 4. Overview of experiments where OAc is added to a CdSe/black Se synthesis run with (red) DAc and (black) OAc. (a) Absorption spectra of the final product of every synthesis. (b) Final nanocrystal diameter in function of the amount of extra OAc in the synthesis. The long wavelength shoulders in the 1:0:3 and 1:3:3 spectra are due to nanocrystal fusion (see Supporting Information, Section S2). (c) Size dispersion of the nanocrystals formed as a function of the amount of extra OAc added. See Methods Section for details on the synthesis and the determination of the nanocrystal diameter and size dispersion.

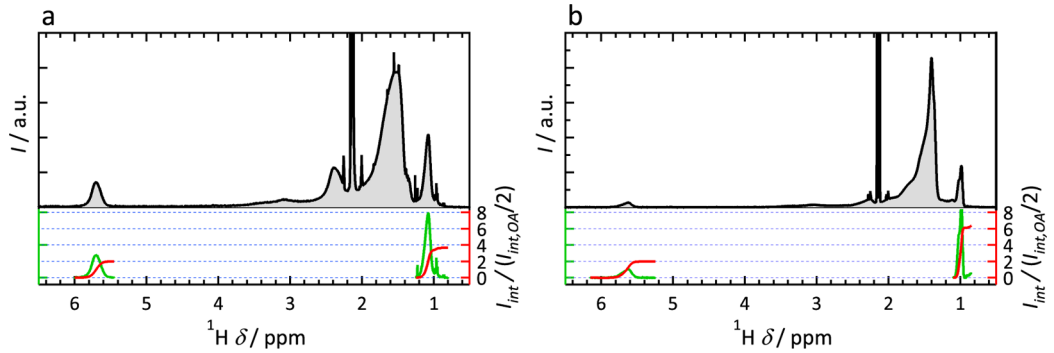

Figure 5. 1D ^{1}H NMR spectra of purified CdSe nanocrystal dispersions synthesized with the CdSe/black Se synthesis using (a) OAc and (b) a 1:1 OAc:DAc ligand mixture. The bottom graphs show (green) the background corrected resonances of the alkene (≈ 5.85 ppm) and methyl (≈ 1.1 ppm) protons and (red) the concomitant integrated intensity. Intensities (green axis) are not in the same scale in (a) and (b). Integrated intensities are normalized at half the integrated intensity of the alkene protons. The nanocrystal diameter amounts to 2.7 and 3.2 nm for the OAc and the OAc:DAc synthesis, respectively, and both NMR spectra were recorded in toluene-d_8 at 298.15 K.

observed size and size distribution tuning to one of these modeling parameters by means of well-designed experiments.

Solute Solubility Changes Cannot Be the Only Explanation for Size Tuning by the Carboxylic Acid Chain Length. In the case of the CdSe/black Se synthesis, carboxylic acids are the only ligand used in the reaction. One can therefore assume that carboxylic acids or carboxylates will coordinate the solute and render it soluble. The same description has been put forward for the solute formed in reactions similar to the CdSe/TOPSe reaction used here.[13,16] The fact that the solubility of carboxylic acids in apolar solvents goes down with increasing chain length,[31] thus brings us to the assumption that also the solubility of the CdSe solute should decrease with increasing chain length. This provides a first possible interpretation of the observed size tuning at constant reaction rate since an increase of the solute solubility results in the formation of larger nanocrystals with a broader size distribution at the end of the reaction.[16]

To investigate this hypothesis, we progressively added OAc to a DAc-based CdSe/black Se synthesis, while keeping the amount of DAc constant. If the observed size-tuning effect would only be related to the CdSe solute solubility, we expect to observe an increasing particle size and size distribution when increasing the OA ligand concentration in line with various previous literature studies.[14,16,32] Figure 4a represents the absorption spectra recorded on the final reaction product for all syntheses, whereas Figure 4b,c shows the final d_{NC} and σ_d of the CdSe nanocrystals obtained from these spectra as a function of the (relative) amount of OAc used. One sees that rather than increasing d_{NC} and σ_d, the addition of OAc to a DAc-based synthesis systematically reduces both d_{NC} and σ_d. These trends strongly contrast with the increase of both parameters when the amount of OAc in an OAc-based synthesis is raised (black markers in Figure 4a,b), a behavior in line with previous literature findings.[16] We thus conclude that changing the ligand chain length in a hot injection synthesis affects other parameters, next to the solute solubility, that have an influence on the balance between the nucleation and growth rate.

Surface Tension and the Surface Reaction Are Not the Driving Force Behind Size Tuning by the Carboxylic Acid Chain Length. The surface tension corresponds to the free energy per surface area of the nanocrystals formed. As such, it can depend on the nature of the adsorbed ligands, where both the binding of the ligands to the nanocrystal and the mutual, interligand van der Waals interactions between the ligands may contribute. By changing the carboxylic acid chain length, the interligand interactions change, which may affect the nanocrystal surface tension. According to Table 1, this could account for the observed link between larger nanocrystals and shorter ligands (see also Supporting Information, Section S3.2) provided that a reduction of the ligand length increases the surface tension. However, in the case that shorter ligands indeed lead to a higher surface tension, free energy

DOI: 10.1021/ja509941g
J. Am. Chem. Soc. 2015, 137, 2495−2505

minimization dictates that syntheses in ligand mixtures should result in nanocrystal surfaces enriched in the longer ligand.

To verify this, we determined the ligand shell composition by solution NMR of two batches of CdSe nanocrystals synthesized using the CdSe/black Se reaction using either pure OAc or a 1:1 OAc:DAc mixture. Figure 5 shows the ^{1}H NMR spectra recorded on both types of nanocrystals dispersed in toluene-d_8. In the case of the OAc only sample (Figure 5a), we obtain a ratio between the integrated intensities of the alkene and methyl protons at, respectively, 5.72 and 1.07 ppm of 2:3.5, which is close to the expected 2:3 for pure OAc. For the CdSe nanocrystals synthesized in the 1:1 OAc:DAc mixture, this intensity ratio increases to 2:6.1. Including the errors related to the background correction, this corresponds to a OAc and DAc fraction in the ligand shell of 0.53 ± 0.05 and 0.47 ± 0.05, respectively. This number closely corresponds to the composition of the reaction mixture. We therefore conclude that there is little enrichment of the ligand shell in either of the two ligands, meaning that the ligand chain length has no significant effect on the nanocrystal surface tension. This paradoxical outcome can be understood by acknowledging that the surface tension is actually the surface contribution of the free energy difference between a nanocrystal and its dissolved constituents, i.e., solute and ligands. Although the interligand van der Waals interactions will be reduced for shorter ligands, so will be the van der Waals interactions between the ligands and the solvent. The absence of preferential adsorption indicates that both contributions largely cancel when their difference is considered.

Considering the rate constant for solute adsorption k_g^∞, an argument often found in the literature is that shorter ligands make the surface more accessible for the solute, thus resulting in larger rate constants for solute adsorption and desorption.[18,21,26] According to Table 1, this should indeed lead to larger nanocrystals since it favors growth over nucleation although k_g^∞ only has a pronounced influence on d_{NC} in a kinetic growth regime, where $D/k_g^\infty \gg r$. The simulations however only reproduce experimental diameters and size dispersions when run in or close to diffusion limitation, with the ratio D/k_g^∞ amounting to 1/50 nm for the standard simulation shown in the Supporting Information (Section S3.3). Moreover, increasing k_g^∞ will only push the synthesis further into diffusion limitation. This means that the more the chain length of the carboxylic acids is reduced, the smaller the additional increase of d_{NC} will be and the more narrow the size dispersion (see Supporting Information, Section S3.3). Since neither of both trends agrees with the experimental results, we conclude that the acid chain length has either no influence on k_g^∞ or that this influence does not affect d_{NC} since nanocrystal growth in the syntheses studied is in or close to diffusion control.

Change of the Diffusion Coefficient of the Solute Is Proportional to the Change of the Diffusion Coefficient of the Carboxylic Acid Ligand. As argued before, it can be assumed that the carboxylic acids used in the CdSe/TOPSe or CdSe/black Se synthesis will coordinate the solute that is formed out of the precursors. As a result, changing the hydrocarbon chain length may also affect the diffusion coefficient of the solute, which is a parameter entering the expression for the nanocrystal growth rate. To assess the possible change in diffusion coefficient one could expect, we used diffusion ordered ^{1}H NMR spectroscopy to determine the diffusion coefficient of $Cd(OAc)_2$ and different carboxylic acids at room temperature in toluene-$d8$. As can be seen in Figure 6, the diffusion coefficient decreases with increasing chain length.

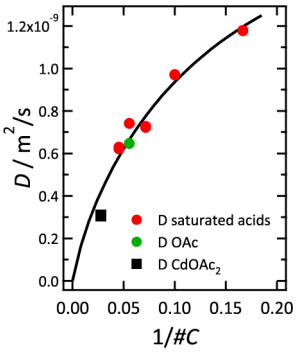

Figure 6. Diffusion coefficients of (red circles) different saturated carboxylic acids, (green marker) OAc and (black marker) cadmium oleate determined at 298.15 K in toluene-d_8 using diffusion ordered ^{1}H NMR spectroscopy as a function of the reciprocal of the number of carbon atoms in the respective hydrocarbon chains. The black line is a fit to the expression for the diffusion coefficient of a freely rotating ellipsoid. See Supporting Information, Section S4, for more details.

Moreover, the obtained diffusion coefficients follow a trend expected for freely rotating rod-like objects (for a detailed discussion see Supporting Information, Section S4), where for long rods, the diffusion coefficient becomes proportional to the rod length. In this respect, we find that the diffusion coefficient of OAc is approximately twice as large as the one of $Cd(OA)_2$, meaning that $Cd(OA)_2$ can roughly be described as an object that is twice as long as one OAc molecule. Hence when indeed carboxylic acids coordinate the solute, this result indicates that we can directly link a change in the carboxylic acid chain length to a variation of the diffusion coefficient of the solute.

Reaction Simulations Confirm the Relation between the Solute Diffusion Coefficient and the Nanocrystal Diameter. Returning to eqs 1 and 2, one sees that the solute diffusion coefficient enters in both the prefactor of the nucleation rate and the expression for the growth rate. Linking the solute diffusion coefficient to the ligand chain length, this provides two possible routes by which the ligand chain length can affect the balance between nucleation and growth. Increasing the nucleation prefactor to accommodate for shorter ligands (and thus a higher diffusion coefficient) results in smaller nanocrystals (see Table 1 and Supporting Information, Section S3.1). However, since only a small change in supersaturation is needed to offset the increased prefactor and obtain the same nucleation rate, the effect is negligible. Moreover, inspecting the assumptions made in deriving eq 1, it follows that the solute diffusion coefficient enters the prefactor only to assess the dissolution rate of critical nuclei.[33] Writing the nucleation prefactor in terms of the solute diffusion coefficient should therefore be seen as a way to estimate its order of magnitude and not as a true functional relation between both. Therefore, we conclude that changing the ligand chain length may well affect the solute diffusion coefficient but will not influence d_{NC} through the (apparent) dependence of the nucleation prefactor on D.

As can be seen in eq 2, the solute diffusion coefficient also directly influences the nanocrystal growth rate, especially for reactions run close to or in diffusion control. Here, an increase of D raises the growth rate, and the concomitantly faster takeover of nucleation by growth makes that less nuclei form

DOI: 10.1021/ja509941g
J. Am. Chem. Soc. 2015, 137, 2495−2505

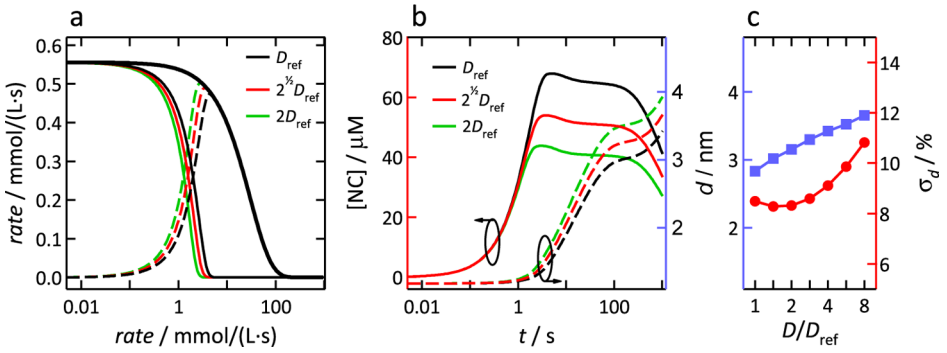

Figure 7. (a) Rates of (bold lines) solute generation, (full lines) solute consumption by nucleation, and (dashed line) solute consumption by growth for simulations of the hot injection synthesis based on a comprehensive model incorporating nucleation and growth of nanocrystals out of solute generated from the injected precursors. Three different diffusion coefficients for the solute are used, (black) $D_{ref} = 0.25 \times 10^{-9}$ m^2/s, (red) $\sqrt{2}D_{ref}$, and (green) $2D_{ref}$. (b) Time development of the concentration and the diameter of the nanocrystals for the three reaction simulations. The same color code is used to indicate simulations with different diffusion coefficients. (c) Representation of (blue squares) diameter and (red circles) size dispersion after 90 s of reaction time as a function of the solute diffusion coefficient, represented as D/D_{ref} on a logarithmic axis.

such that they can grow larger by the end of the reaction. Figure 7 shows the results of reaction simulations implementing eqs 1 and 2 that clarify this point (see Supporting Information, Sections S2 and S3.4). The reference synthesis shown in black is based on a parameter set that makes the simulated reference reaction have a comparable rate and a similar d_{NC} as the experimental syntheses studied here. First of all, Figure 7a shows the different rates involved in the formation and consumption of solute. In line with the argument made previously, one sees that all solute species formed (bold line) are initially consumed by nucleation (full line), which is later overtaken by consumption through growth (dashed line). After the suppression of the nucleation, the nanocrystal concentration [NC] is maintained at an approximately steady value and d_{NC} increases to level off when the reaction reaches full yield (see Figure 7b). After that, Ostwald ripening results in a drop of the nanocrystal concentration and a further growth of the remaining nanocrystals.

Next to the reference simulation, where a diffusion coefficient D_{ref} of 0.25×10^{-9} m^2/s is used, the figure also shows simulation results where D has been multiplied by a factor of $\sqrt{2}$ and 2. Figure 7a indicates that a higher diffusion coefficient indeed speeds up the takeover of nucleation by growth. In line with the qualitative statements in Table 1, this results in a lower concentration of nanocrystals after nucleation is suppressed, and the nanocrystals attain larger diameters when the reaction reaches full yield (Figure 7b). Quantitatively, we find that a doubling of the diffusion coefficient relative to the reference conditions raises d_{NC} by ≈0.5 nm, and Figure 7c indicates that this increase continues when raising D even further. Importantly, this predicted change is in line with the changes found experimentally when comparing syntheses run using DAc (C10) or BAc (C22), where a difference in diffusion coefficient of ≈2 can indeed be expected. Figure 7c also lists σ_d at the point where the reaction reaches full yield. One sees that an initial increase of D relative to the D_{ref} has little effect on σ_d. On the other hand, raising D further leads to a progressive increase of σ_d, in line with what was reported before for a solubility increase.[16] This trend can be understood from eq 2, which makes clear that increasing D will shift the growth from diffusion to kinetic control, thus reducing size distribution focusing. We thus conclude that at least part of the increase of d_{NC} observed when reducing the chain length of the carboxylic acids in the CdSe/TOPSe and CdSe/black Se synthesis can be due to an increase of the solute diffusion coefficient.

Size Tuning by the Carboxylic Acid Chain Length Results from Changing the Solute Diffusion Coefficient and Solubility. Various studies on the synthesis of metal, metal oxide, or semiconductor nanocrystals have mentioned that a reduction of the ligand chain length—being either carboxylic acids, amines, phosphines, or phosphine oxides—leads to larger nanocrystals.[18−26] When discussed, this effect has been attributed to an overall slowing down of nucleation and growth for longer chains, tentatively linked to an increase of steric hindrance.[18,21,26] Opposite from this interpretation, we find for the two different CdSe syntheses studied here that a change of the ligand chain length has no noticeable influence on the reaction rate. If the combined rate of solute consumption by nucleation and growth remains the same, the observed size tuning can only be due to a change of the moment where the increasing consumption of solute by nanocrystal growth suppresses the nucleation of new nanocrystals. Although the different composition of the ligand shell could play a role here, either through a variation of the solute adsorption rate k_g^∞ or the surface free energy γ, only a change of the solute diffusion coefficient D and the solute solubility $[M]_0$ yield the experimentally observed combined increase of the nanocrystal diameter d_{NC} and size dispersion σ_d when simulating the reactions.

Including the experimental results shown in Figures 3 and 4, both relations explain why the use of pure acids or acid mixtures with the same average chain length yield the same nanocrystal diameter. When the carboxylic acids coordinate the solute, both its solubility and its diffusion coefficient will indeed be an average taken over the different carboxylic acids used. On the other hand, only the connection between the ligand chain length and the solute diffusion coefficient can explain why d_{NC} goes down when OAc is added to a synthesis run using DAc only. In that case, the solubility is supposed to go up, leading to larger nanocrystals, hence the slight increase in d_{NC} observed when more OAc is added to a synthesis already run using OAc. On the other hand the replacement of DAc by OAc as a coordinating species for the solute will reduce its diffusion coefficient by about a factor of 2, which explains the experimentally observed marked drop in d_{NC}. However, one sees that in particular for the CdSe/black Se synthesis the actually measured change in d_{NC} as a function of the acid chain

DOI: 10.1021/ja509941g
J. Am. Chem. Soc. 2015, 137, 2495−2505

length exceeds the variation expected from the simulations. When D is raised by about a factor of 2 (DAc versus BAc), d_{NC} increases by ≈1 nm, whereas only ≈0.5 nm is predicted. Since D and $[M]_0$ play a very similar role in the reaction simulations (see Supporting Information, Sections S3 and S4), this indicates that the increase of d_{NC} most likely results from the joint increase of the diffusion coefficient and the solubility of the solute when reducing the chain length of the carboxylic acids.

Dative Ligands Do Not Change the Diffusion Coefficient and Show Little Effect of Chain Length on Size and Size Distribution in a Regime of Ideal Dilution. The conclusion that the ligand chain length influences d_{NC} through its effect on the diffusion coefficient or the solubility of the solute suggests that a change in diameter will occur only if the ligands interact to some extent with the solute, either through direct (inner sphere) or a more loose (outer sphere) coordination. Formulated in this way, one sees that the chain length/d_{NC} relation could be used to probe possible interactions between a reaction additive and the solute. Considering the binding of ligands to nanocrystals such as CdSe, it has been well established that carboxylic acids adsorb as tightly bound, X-type carboxylate species.[34,35] Amines on the other hand are dative L-type ligands that are more loosely bound and exhibit a rapid adsorption/desorption behavior.[36] This different coordination behavior at the level of the nanocrystals raises the question as to how the diffusion coefficient of the solute and thereby the size- and size-distribution development of nanocrystals during a synthesis will be affected by a change of the ligand chain of a dative, L-type ligand. To analyze this, we studied the yield, size, and size distribution development of the CdSe/TOPSe syntheses using saturated, primary amines with different chain lengths. Here, the concentration of the amine was kept comparatively low so that it can be assumed that changes of the solubility will play a minor role.[16]

As shown in Figure 8a, we again find the same yield development for different CdSe/TOPSe syntheses run using *n*-dodecylamine (C12), *n*-tetradecylamine (C14), *n*-hexadecylamine (C16), and *n*-octadecylamine (C18). Hence, changing the amine chain length has no effect on the reaction rate. In this case, however, also the absorption spectra recorded on aliquots taken after 8 min of reaction time show little variation, if any (see Figure 8b). We thus conclude that the outcome of the CdSe/TOPSe synthesis is almost independent of the chain length of the amine used. In line with this finding, Figure 8c shows the room temperature diffusion coefficient of $Cd(OAc)_2$ dissolved in toluene, again determined using DOSY, with and without the presence of octadecylamine (ODA, C18). Clearly, ODA has no influence on this diffusion coefficient within the precision of the measurement. This correspondence—albeit recorded on $Cd(OAc)_2$ and not on the actual solute—further supports the interpretation put forward that the strong effect of the ligand chain length on the nanocrystal diameter observed for carboxylic acids is related to the acid coordinating the solute and thus changing its diffusion coefficient. With additives such as amines that show far less interaction with the solute, no influence of the chain length on the final nanocrystal size is observed (see Figure 8d).

Ligands with a Shorter Hydrocarbon Chain Lead to a Higher Solubility. Besides the diffusion coefficient effect, we have already mentioned that carboxylic acids with a shorter hydrocarbon chain are more soluble in apolar solvents.[17]

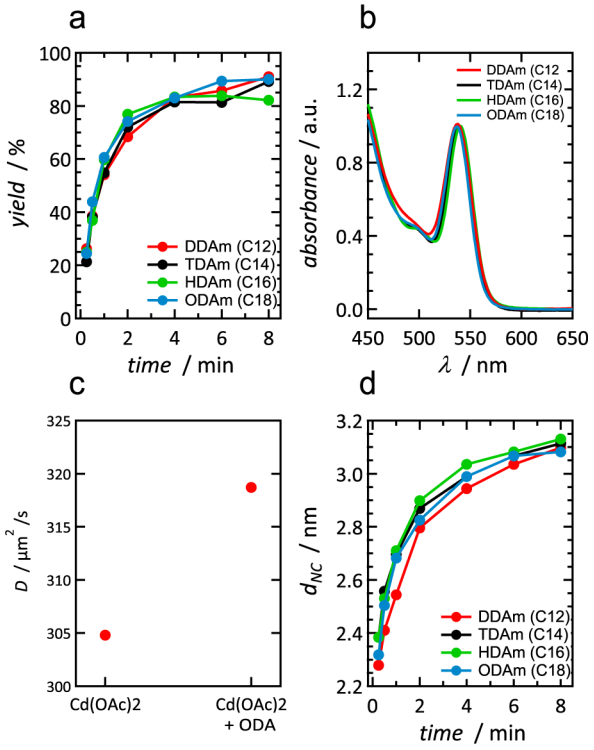

Figure 8. (a) Time development of the reaction yield of CdSe/TOPSe syntheses run using primary amines with different hydrocarbon chain length, including dodecylamine (DDAm), tetradecylamine (TDAm), hexadecylamine (HDAm), and octadecylamine (ODAm). (b) Absorption spectra recorded on aliquots taken 8 min after injection for the different reactions shown in (a). (c) Diffusion coefficient of $Cd(OA)_2$ in toluene-d_8 at 298.15 K with and without octadecylamine present. (d) Time development of the nanocrystal diameter for the different reactions shown in (a).

Although this was ruled out as the sole origin of the observed size tuning (see Figure 4), we already concluded that an increase of the solubility still contributes to the observed size tuning when changing the carboxylic acid chain length. It leads to the same observations, namely an increase of the particle size and size distribution when using ligands with shorter hydrocarbon chains[16] and the experimental increase of d_{NC} is larger than expected for the given change in diffusion coefficient. To address this aspect separately and, in doing so, extend the study to yet another ligand systems, trialkylphosphine oxides were added to the CdSe/TOPSe synthesis, where both tributylphosphine oxide (TBPO) and trioctylphosphine oxide (TOPO) were used (see Supporting Information, Section S6, for an analysis of the phosphine oxide purity). For both additives, we always analyzed d_{NC} and σ_d attained at the end of the reaction.

Similar to all other reactions studied, we find that the yield development is independent of both the concentration and the type of phosphine oxide added (see Supporting Information S6). As shown in Figure 9a,b, we find only a minor effect on d_{NC} and σ_d for low phosphine oxide concentrations that is independent of the phosphine oxide used. This lack of influence of the chain length resembles what is found with amines (see Figure 8b), suggesting that the main effect is rather due to a change of the solubility of the solute and not its diffusion coefficient. With increasing phosphine oxide concentration, the particles grow larger and the size distribution broadens, indicating a further increase of the solubility of the

DOI: 10.1021/ja509941g
J. Am. Chem. Soc. 2015, 137, 2495−2505

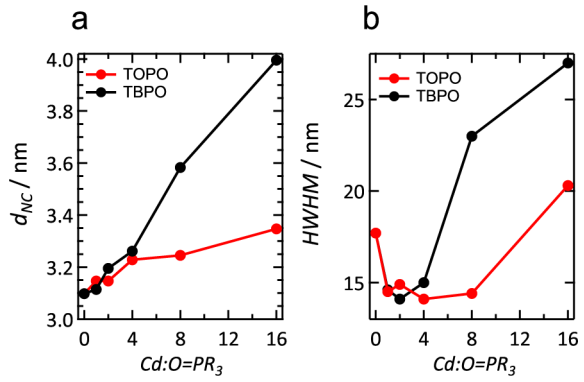

Figure 9. Overview of (a) nanocrystal diameter and (b) spectral width after 8 min reaction time in function of the cadmium to trialkylphosphine oxide ratio inside the reaction mixture for a CdSe/TOPSe-based reaction. Reaction mixture: 0.2 mmol Cd(OA)2, 0.8 mmol OA, 1.6 mmol HDA, and the particular amount phosphine oxide (total mass 8 g). Injection mixture: 2 mL 1 M TOPSe. Injection and growth temperature: 245 and 230 °C, respectively.

solute inside the reaction mixture.[16] Furthermore, this effect is stronger for TBPO than for TOPO, which indicates that indeed the solubility will increase more when the hydrocarbon chain-length of the alkylphosphine oxides is shorter. We thus conclude that the ligand chain length can also affect the nanocrystal size and size distribution in a hot injection synthesis by its effect on the solubility of the solute. Given the deterioration of the size dispersion with increasing solubility, this makes long chained ligands favorable in strongly coordinating reaction mixtures since they have a lower impact on the solubility of the solute.

CONCLUSION

We have analyzed the relation between the hydrocarbon chain length of ligands added to a hot injection synthesis and the diameter of the nanocrystals thus formed at the end of the reaction. In the case of carboxylic acids, we find for two different syntheses for CdSe nanocrystals that shorter chain lengths result in larger nanocrystals, where especially for the shortest ligands used the size dispersion also deteriorates. This finding is in line with various literature reports, yet opposite from the prevailing explanation that longer ligands slow down the reaction, we find that the ligand chain length has no effect on the reaction rate. Based on a combination of experimental evidence and reaction simulation, we therefore attribute the observed size tuning to a change of the moment where nanocrystal nucleation is overtaken by nanocrystal growth, due to the carboxylic acids affecting both the diffusion coefficient and the solubility of the solute species formed out of the injected precursors. This conclusion suggests that the chain length/d_{NC} relation could be used to probe the degree of interaction between a reaction additive and the solute, a point we explored further by changing the chain length of amines and phosphine oxides. Especially in the case of amines, the ligand chain length has no noticeable effect on d_{NC}, suggesting little interaction with the solute in line with the weak, dynamic stabilization of CdSe nanocrystals by amines. Hence, this study shows that changing the ligand chain length provides a practical way to tune the nanocrystal diameter at full yield in a hot injection synthesis and enhance the size dispersion, which is key to the application of nanocrystals as light emitters, for example, in display applications. Moreover, the ligand chain length can be used to probe the interaction between a reaction additive and the solute, which can lead to better insight in the hot injection synthesis itself.

METHODS

CdSe/TOPSe Reference Synthesis. CdSe QDs were synthesized following a previously described procedure.[15] In brief, a mixture of cadmium oleate (0.2 mmol), HDA (1.6 mmol), OAc (variable amount, molar ratio Cd:OA:HDA 1:*x*:8 as indicated), and ODE (total volume = 10 mL) were stirred under a nitrogen flow for 30 min at room temperature and 60 min at 100 °C. The nitrogen flow was stopped, and still under nitrogen, the temperature was raised to 245 °C and 2 mL of a 1 M TOPSe solution (2 mmol) was injected, and the reaction was performed at 230 °C. Aliquots were taken after specific reaction times, weighed, dissolved in a 1:5 mixture of OA and toluene, precipitated, and resuspended using methanol and toluene as the nonsolvent and the solvent, respectively. For the synthesis work, toluene (>99.8%), methanol (>99.85%), and 2-propanol (>99.7%) were purchased from Fiers; OAc (90%) and cadmium oxide (CdO; > 99.99% metals bases) were purchased from Sigma-Aldrich; selenium (99.999%) and 1-octadecene (ODE; tech.) were purchased from Alfa Aesar; hexadecylamine (HDA, 90%) was purchased from Merck; and trioctylphospine (TOP, 97%) was purchased from Strem.

CdSe/TOPSe Synthesis Using Different Amines and Phosphine Oxides. To investigate the effect of dative ligands, CdSe QDs were synthesized similarly to the synthesis mentioned above where cadmium oxide (0.2 mmol) and OAc (0.8 mmol) were mixed with ODE. The amount of ODE was adjusted in the way that the mass of all constituents inside the reaction mixture, after adding amines and phosphine oxides, was 8 g. This mixture was evacuated for 1 h at 110 °C, set under nitrogen and heated up until the mixture turned clear, cooled down to room temperature, opened, and the particular amine (1.6 mmol) and phosphine oxide were added without further purification. The mixture was set again under vacuum, evacuated at 110 °C for 1 h, and set under nitrogen, and the temperature was raised to 245 °C. Then 2 mL of a 1 M TOPSe solution (2 mmol) were injected, and the reaction was performed at 230 °C. Aliquots were taken after specific reaction times, weighed, dissolved in toluene, precipitated, and resuspended twice using ethanol and isopropanol as nonsolvents and toluene as solvent. For the synthesis work, toluene (CP), ethanol (>96%), and 2-propanol were purchased from Gadot; 2-propanol (CP) was purchased from Bio-Lab; OAc (90%), ODE (tech.), cadmium oxide (CdO; > 99.99% metals bases), selenium (99.999%), HDA (tech.), TOPO (99%), and TBPO were purchased from Sigma-Aldrich; dodecylamine (DDA, > 98%), tetradecylamine (TDA, > 99%), and octadecylamine (ODA, tech.) were purchased from Fluka; and trioctylphospine (TOP, 97%) was purchased from Strem.

CdSe/Black Se Synthesis. CdSe QDs were synthesized following a previously described procedure.[22] CdO (0.4 mmol) was added to 10 mL of ODE together with 1.2 mmol of myristic acid in a three-neck flask with cooler under air. The mixture was heated up to 270 °C to form a cadmium carboxylate complex. The heterogeneous ODE-Se precursor was prepared by adding 0.2 mmol of Se powder to 1 mL of ODE at room temperature. The resulting unstable dispersion was left stirring, yet no attempt was made to dissolve the Se powder by heating. To initiate the reaction, the heterogeneous ODE-Se precursor was swiftly injected in the colorless reaction mixture containing the Cd precursor. Injection and growth temperatures were set at 270 and 260 °C, respectively. The black color of the heterogeneous ODE-Se precursor disappeared upon injection, and the color of the mixture turned from yellow to orange to red depending on the size of the CdSe nanocrystals formed. For quantitative measurements, aliquots were taken after specific reaction times, weighed, dissolved in a 1:5 mixture of OA and toluene, precipitated, and resuspended using methanol and toluene as the nonsolvent and the solvent, respectively. The reaction was stopped by thermal quenching using a water bath. The reaction mixture was purified by the addition of toluene, isopropanol, and methanol, both in a 1:1:1 ratio relative to the volume

DOI: 10.1021/ja509941g
J. Am. Chem. Soc. 2015, 137, 2495−2505

of the reaction mixture. The resulting turbid solution was centrifuged to obtain a precipitate of NCs that was redispersed in toluene. Prior to a second purification step, OAc was added in a 10:1 ratio relative to the amount of acid originally used in the synthesis to replace the original carboxylic acid on the surface of the nanocrystals. Next, the purification was repeated twice using, respectively, toluene and methanol as solvent and nonsolvent to remove all residual reaction products. For the synthesis work, the same products were used as for the CdSe/TOPSe Synthesis.

Analysis of Absorption Spectra. UV−vis spectra of purified, weighted aliquots were recorded for quantitative analysis with a PerkinElmer Lambda 2 spectrophotometer.[15] Using the zb-CdSe sizing curve,[29] the mean QD diameter, d_{NC}, is calculated from the peak wavelength of the first exciton transition. The amount of CdSe formed n_{CdSe} is obtained from the average absorbance of a diluted aliquot at 300, 320, and 340 nm, which is directly proportional to the volume fraction of CdSe.[29] The size distribution is estimated from the half-width at half-maximum of the absorption peak of the first exciton transition. In the case of a double size distribution due to nanocrystal fusion, the size dispersion plotted is that of the primary set of (not fused) nanocrystals, where the half-width at half-maximum is estimated by fitting a sum of two Gaussians to the first exciton peak (see Supporting Information, Section S2).[16]

Nuclear Magnetic Resonance Spectroscopy. NMR samples of purified NC dispersions are prepared by evaporation of the toluene with a strong nitrogen flow in the glovebox. The resulting dry NCs are dissolved in deuterated toluene-d_8 (99,50% D, purchased at Eurisotop) and transferred to an NMR tube (5 mm). NMR measurements were recorded on a Bruker Avance III Spectrometer operating at a ^{1}H frequency of 500.13 MHz and equipped with a BBI-Z probe or on a Bruker Avance II Spectrometer operating at a ^{1}H frequency of 500.13 MHz and equipped with a TXI-Z probe (channels are ^{1}H, ^{1}3C, ^{3}1P). The sample temperature was set to 298.15 K. Quantitative ^{1}H spectra were recorded with a 20 s delay between scans to allow full relaxation of all NMR signals. The quantification was done by using the Digital ERETIC method. Diffusion measurements (2D DOSY) were performed using a double stimulated echo sequence for convection compensation and with monopolar gradient pulses.[37] Smoothed rectangle gradient pulse shapes were used throughout. The gradient strength was varied linearly from 2 to 95% of the probes maximum value (calibrated at 50.2 G/cm) in 64 steps, with the gradient pulse duration and diffusion delay optimized to ensure a final attenuation of the signal in the final increment of <10% relative to the first increment. For 2D processing, before Fourier transformation, the 2D spectra were multiplied with a squared cosine bell function in both dimensions. The alkene and methyl proton resonances were corrected prior to integration by subtracting a linear background from the measured intensity.

Reaction Simulations. Modeling of the QD synthesis was done by implementing the equations given in the Supporting Information, into COMSOL Multiphysics, a commercially available finite-element partial differential equation solver. The parameters used for the reference simulation are given in the Supporting Information, Section S2.2.

■ ASSOCIATED CONTENT

Supporting Information

An overview of all absorption spectra of reaction aliquots; data on the black Selenium synthesis executed at 270/260 °C injection/growth temperature; background to the simulations of the hot injection synthesis, including the model equations and the standard parameter set; detailed simulation results showing the influence of the nucleation prefactor, the surface tension, the adsorption rate constant, the solute diffusion coefficient, and the solute solubility on the diameter and the size dispersion of the nanocrystals; the analysis of the diffusion coefficient of carboxylic acids and cadmium oleate in toluene; and yield developments of the TOP-Se synthesis with addition of phosphine oxides. This material is available free of charge via the Internet at http://pubs.acs.org/.

■ AUTHOR INFORMATION

Corresponding Authors

*capek@techunix.technion.ac.il

*zeger.hens@ugent.be

Author Contributions

⊥These authors contributed equally.

Notes

The authors declare no competing financial interest.

■ ACKNOWLEDGMENTS

Z.H. acknowledges Ghent University (BOF-GOA), the FWO-Vlaanderen (G.0760.12), BelSPo (IAP 7.35, photonics@be), and H2020 MSCA actions (ETN phonsi) for funding. S.A. acknowledges the IWT-Vlaanderen (Agency for Innovation by Science and Technology in Flanders) for a scholarship.

■ REFERENCES

(1) Talapin, D. V.; Lee, J.-S.; Kovalenko, M. V.; Shevchenko, E. V. *Chem. Rev.* **2010**, *110*, 389−458.

(2) Murray, C.; Kagan, C.; Bawendi, M. *Annu. Rev. Mater. Sci.* **2000**, *30*, 545−610.

(3) Murray, C.; Norris, D.; Bawendi, M. *J. Am. Chem. Soc.* **1993**, *115*, 8706−8715.

(4) Peng, Z.; Peng, X. *J. Am. Chem. Soc.* **2001**, *123*, 183−184.

(5) Peng, X.; Manna, L.; Yang, W.; Wickham, J.; Scher, E.; Kadavanich, A.; Alivisatos, A. *Nature* **2000**, *404*, 59−61.

(6) Carbone, L.; Nobile, C.; De Giorgi, M.; Sala, F. D.; Morello, G.; Pompa, P.; Hytch, M.; Snoeck, E.; Fiore, A.; Franchini, I. R.; Nadasan, M.; Silvestre, A. F.; Chiodo, L.; Kudera, S.; Cingolani, R.; Krahne, R.; Manna, L. *Nano Lett.* **2007**, *7*, 2942−2950.

(7) Donega, C. d. M. *Chem. Soc. Rev.* **2011**, *40*, 1512−1546.

(8) Garcia-Rodriguez, R.; Hendricks, M. P.; Cossairt, B. M.; Liu, H.; Owen, J. S. *Chem. Mater.* **2013**, *25*, 1233−1249.

(9) Sowers, K. L.; Swartz, B.; Krauss, T. D. *Chem. Mater.* **2013**, *25*, 1351−1362.

(10) Hens, Z.; Capek, R. K. *Coordin. Chem. Rev.* **2014**, *263−264*, 217−228.

(11) Steckel, J. S.; Yen, B. K. H.; Oertel, D. C.; Bawendi, M. G. *J. Am. Chem. Soc.* **2006**, *128*, 13032−13033.

(12) Allen, P. M.; Walker, B. J.; Bawendi, M. G. *Angew. Chem., Int. Ed.* **2010**, *49*, 760−762.

(13) Liu, H.; Owen, J. S.; Alivisatos, A. P. *J. Am. Chem. Soc.* **2007**, *129*, 305−312.

(14) Owen, J. S.; Chan, E. M.; Liu, H.; Alivisatos, A. P. *J. Am. Chem. Soc.* **2010**, *132*, 18206−18213.

(15) Abe, S.; Capek, R. K.; De Geyter, B.; Hens, Z. *ACS Nano* **2012**, *6*, 42−53.

(16) Abe, S.; Capek, R. K.; De Geyter, B.; Hens, Z. *ACS Nano* **2013**, *7*, 943−949.

(17) Hoerr, C. W.; Sedgwick, R. S.; Ralston, A. W. *J. Org. Chem.* **1946**, *11*, 603−609.

(18) Battaglia, D.; Peng, X. G. *Nano Lett.* **2002**, *2*, 1027−1030.

(19) Lucey, D. W.; MacRae, D. J.; Furis, M.; Sahoo, Y.; Cartwright, A. N.; Prasad, P. N. *Chem. Mater.* **2005**, *17*, 3754−3762.

(20) Baek, I. C.; Il Seok, S.; Pramanik, N. C.; Jana, S.; Lim, M. A.; Ahn, B. Y.; Lee, C. J.; Jeong, Y. J. *J. Colloid Interface Sci.* **2007**, *310*, 163−166.

(21) Ouyang, J.; Kuijper, J.; Brot, S.; Kingston, D.; Wu, X.; Leek, D. M.; Hu, M. Z.; Ripmeester, J. A.; Yu, K. *J. Phys. Chem. C* **2009**, *113*, 7579−7593.

(22) Flamee, S.; Cirillo, M.; Abe, S.; De Nolf, K.; Gomes, R.; Aubert, T.; Hens, Z. *Chem. Mater.* **2013**, *25*, 2476−2483.

DOI: 10.1021/ja509941g
J. Am. Chem. Soc. 2015, 137, 2495−2505

(23) Nose, K.; Fujita, H.; Omata, T.; Otsuka-Yao-Matsuo, S.; Nakamura, H.; Maeda, H. *J. Lumin.* **2007**, *126*, 21−26.
(24) Sun, S. H.; Murray, C. B. *J. Appl. Phys.* **1999**, *85*, 4325−4330.
(25) Green, M.; Allsop, N.; Wakefield, G.; Dobson, P. J.; Hutchison, J. L. *J. Mater. Chem.* **2002**, *12*, 2671−2674.
(26) Epifani, M.; Arbiol, J.; Diaz, R.; Peralvarez, M. J.; Siciliano, P.; Morante, J. R. *Chem. Mater.* **2005**, *17*, 6468−6472.
(27) Chan, E. M.; Xu, C.; Mao, A. W.; Han, G.; Owen, J. S.; Cohen, B. E.; Milliron, D. J. *Nano Lett.* **2010**, *10*, 1874−1885.
(28) Capek, R. K.; Lambert, K.; Dorfs, D.; Smet, P. F.; Poelman, D.; Eychmueller, A.; Hens, Z. *Chem. Mater.* **2009**, *21*, 1743−1749.
(29) Capek, R. K.; Moreels, I.; Lambert, K.; De Muynck, D.; Zhao, Q.; Van Tomme, A.; Vanhaecke, F.; Hens, Z. *J. Phys. Chem. C* **2010**, *114*, 6371−6376.
(30) Talapin, D.; Rogach, A.; Haase, M.; Weller, H. *J. Phys. Chem. B* **2001**, *105*, 12278−12285.
(31) Hoerr, C. W.; Sedgwick, R. S.; Ralston, A. W. *J. Org. Chem.* **1946**, *11*, 603−609.
(32) Bullen, C.; Mulvaney, P. *Nano Lett.* **2004**, *4*, 2303−2307.
(33) Nielsen, A. E. *Kinetics of Precipitation*; Pergamon Press: New York, 1964.
(34) Fritzinger, B.; Capek, R. K.; Lambert, K.; Martins, J. C.; Hens, Z. *J. Am. Chem. Soc.* **2010**, *132*, 10195−10201.
(35) Anderson, N. C.; Owen, J. S. *Chem. Mater.* **2013**, *25*, 69−76.
(36) Hassinen, A.; Moreels, I.; Donega, C. d. M.; Martins, J. C.; Hens, Z. *J. Phys. Chem. Lett.* **2010**, *1*, 2577−2581.
(37) Connell, M. A.; Bowyer, P. J.; Bone, P. A.; Davis, A. L.; Swanson, A. G.; Nilsson, M.; Morris, G. A. *J. Magn. Reson.* **2009**, *198*, 121−131.

DOI: 10.1021/ja509941g
J. Am. Chem. Soc. 2015, 137, 2495−2505